PNAS RESEARCH ARTICLE | CHEMISTRY

Water–solid contact electrification causes hydrogen peroxide production from hydroxyl radical recombination in sprayed microdroplets

Bolei Chen[a,b,c,1], Yu Xia[b,d,1], Rongxiang He[b,e,1], Hongqian Sang[b,e], Wenchang Zhang[b], Juan Li[b,d], Lufeng Chen[b], Pu Wang[b], Shishang Guo[d], Yongguang Yin[c], Ligang Hu[c], Maoyong Song[c], Yong Liang[a,b,2], Yawei Wang[b,c], Guibin Jiang[c], and Richard N. Zare[f,2]

Contributed by Richard N. Zare; received May 26, 2022; accepted June 23, 2022; reviewed by Veronica Vaida and Zhong Lin Wang

Contact electrification between water and a solid surface is crucial for physicochemical processes at water–solid interfaces. However, the nature of the involved processes remains poorly understood, especially in the initial stage of the interface formation. Here we report that H_2O_2 is spontaneously produced from the hydroxyl groups on the solid surface when contact occurred. The density of hydroxyl groups affects the H_2O_2 yield. The participation of hydroxyl groups in H_2O_2 generation is confirmed by mass spectrometric detection of ^{18}O in the product of the reaction between 4-carboxyphenylboronic acid and ^{18}O–labeled H_2O_2 resulting from $^{18}O_2$ plasma treatment of the surface. We propose a model for H_2O_2 generation based on recombination of the hydroxyl radicals produced from the surface hydroxyl groups in the water–solid contact process. Our observations show that the spontaneous generation of H_2O_2 is universal on the surfaces of soil and atmospheric fine particles in a humid environment.

contact electrification | water droplets | hydroxyl radical | hydrogen peroxide | solid–water interface

Significance

Bulk water is a highly stable solvent, but water microdroplets possess strikingly different properties, such as the presence of hydroxyl radicals (•OH) at the microdroplet periphery. Previous studies demonstrated the recombination of •OH into H_2O_2 molecules and the capture of •OH by oxidizing other molecules, but the origin of the •OH has been a controversial topic with clear evidence that •OH can arise from external gases in contact with the microdroplet surface but also from the formation of the microdroplet itself. This study shows that the latter can primarily arise from contact electrification, which is shown to be a universal phenomenon for water–solid interfaces.

When two materials of different chemical composition are brought into intimate contact, it is common for the two materials to become oppositely charged. Early work suggested that this charging was caused by ion transfer, but more recent work, as reviewed by Lin, Chen, and Wang (1), indicates that electron transfer plays a dominant role in liquid–solid contact electrification (CE). Of special interest is CE involving water droplets and insulators, which began in the 1990s with studies by Matsui et al.; Yatsuzuka, Mizuno, et al.; and Yatsuzuka, Higashiyama, et al. (2–4). They found that the water droplet is always positively charged when it slides over an insulator surface. They conjectured that the adsorption of negative ions from water to the insulator surface was responsible for the contact charging between the water and the insulator. More recent work (1, 5) suggests that both electron and ion transfer occur at the liquid–solid interface but that electron transfer may often predominate. In water, if an electron is to be transferred, then it may seem likely that it would originate from the hydroxide anion (OH^-) causing the formation of the hydroxyl radical (•OH), which may go on to recombine with other hydroxyl radicals to generate hydrogen peroxide (H_2O_2). A recent publication by Ben-Amotz predicted that hydrogen bond charge transfer in water may have far-reaching chemical implications (5), and it is proposed that even transfer from H_2O to form H_2O^+ occurs in which the H_2O^+ cation rapidly reacts with water to yield H_3O^+ and •OH (6). While evidence of the formation of H_2O_2 in water droplets seems to have been well established (7–14), some have claimed that it arises solely from the adsorption of ozone (O_3) (10) or solely from cavitation (14). A recent study employing ultrapure nitrogen (N_2) as a nebulizing gas showed, however, that H_2O_2 in sprayed water droplets was formed without the adsorption of ozone (13), although there can be no denying that ozone adsorption promotes H_2O_2 production as does oxygen (O_2) adsorption (13), as is also the case for cavitation. The question has remained unsettled regarding where the electron that forms •OH goes. It has been speculated that the electron may jump onto positively charged droplets, be captured by water at the air–water interface, or go to the walls in some form of contact electrification (13). In what follows, evidence is presented that contact electrification plays a leading role, and that in the case of silica this involves hydroxyl groups on the solid surface in contact with water.

Electron transfer at a water–solid interface is induced by the overlap of electron clouds, which occurs when water molecules collide with atoms or molecules on the solid surface (15, 16). Notably, electron transfer at a water–solid interface can drive catalytic reactions and facilitate pollutant degradation (17). Liquid–solid triboelectric nanogenerators have also been designed based on this observation (1, 18). Despite advances in applications of electron transfer at water–solid interfaces, the exact nature of the physicochemical processes

Author contributions: B.C. and R.H. designed research; Y.X. performed research; B.C., R.H., H.S., W.Z., J.L., L.C., P.W., S.G., Y.Y., L.H., M.S., Y.L., Y.W., G.J., and R.N.Z. analyzed data; and B.C., R.H., and R.N.Z. wrote the paper.

Reviewers: V.V., University of Colorado Boulder; and Z.L.W., Georgia Institute of Technology.

The authors declare no competing interest.

[1]B.C., Y.X., and R.H. contributed equally to this paper.

[2]To whom correspondence may be addressed. Email: ly76@263.net or zare@stanford.edu.

This article contains supporting information online at http://www.pnas.org/lookup/suppl/doi:10.1073/pnas.2209056119/-/DCSupplemental.

Published August 1, 2022.

that accompany charge transfer is poorly understood. Recently, quantum theory calculations have been used to explain the interactions between water and atomically smooth solid surfaces by considering the coupling of water fluctuations to electronic excitations within the solid (19). In practice, atomically smooth solid surfaces do not exist in any material because of the presence of oxygen-containing chemical groups on the solid surface. Surface chemical groups may therefore play an important role in the physicochemical processes involved in electron transfer in the initial stage of water–solid contact, and in the corresponding interfacial redox chemical processes. However, the effects of surface chemical groups on the contact between water and a solid in the initial stage have usually been ignored. In research on water–solid interfaces, it is therefore crucial to understand the correlation between chemical groups and the physicochemical processes that occur in the initial stage of contact, as well as the interfacial redox chemical reaction. This study is hopefully an advance in this direction.

Results and Discussion

Spontaneous Generation of H_2O_2 in the Microfluidic Channel. An ideal water–solid interface was set up by sealing a patterned polydimethylsiloxane (PDMS) slab on a flat glass substrate to produce a typical straight-channel microfluidic chip. The channel dimensions were 100 μm (width) × 20 μm (height). Deionized (DI) water was injected into the microfluidic channel to build a water–solid interface; this ruled out the effects of gas–phase species on the investigation of H_2O_2 spontaneous generation (Fig. 1*A*). An H_2O_2-sensitive water-soluble probe (10-acetyl-3,7-dihydroxyphenoxazine) was used to detect the production of H_2O_2 in the microfluidic chip (20). The resulting microfluidic chip was examined using fluorescence microscopy to establish a relationship between the water–solid interface and observed fluorescence intensity (Fig. 1*B*). A strong orange fluorescence emission was observed from microfluidics containing the probe under 530 nm laser excitation, as shown in Fig. 1*C*, but not in bulk water under the same conditions. A zoomed-in fluorescence microscopy image confirmed a fluorescence emission from the microfluidics in the straight channel (Fig. 1*D*). Fluorescence analysis indicated that H_2O_2 was generated spontaneously in the microfluidic channel. We confirmed that H_2O_2 was generated by collecting the water in the microfluidic channel and investigating its reaction with 4-carbonxyphenylboronic acid (4-CPB) according to a reported method (6). Mass spectrometric analysis (*SI Appendix*, Figs. S1 and S2) showed that typical boronic acid cleavage occurred and confirmed the presence of H_2O_2, in good agreement with previous literature reports (6). Fig. 1*E* and *SI Appendix*, Fig. S3 show the fluorescence emission intensity as

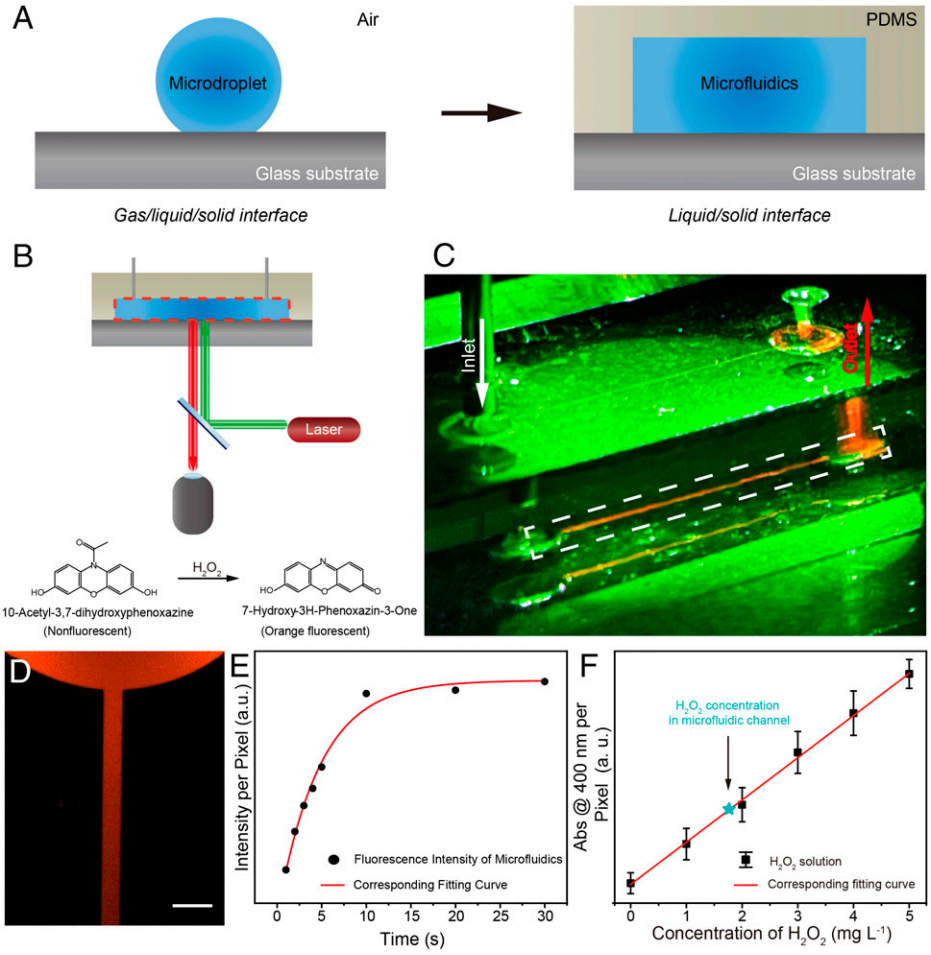

Fig. 1. Fluorescence imaging of spontaneous generation of H_2O_2 in a typical straight-channel microfluidic chip. (*A*) Schematic image of experimental setup of water–solid interface in the microfluidic chip. (*B*) Schematic image of fluorescence microscopy setup for imaging the microfluidic chip. (*C*) Digital image of fluorescence emission of the microfluidic chip. The sample in the chip contains 1 mM H_2O_2-sensitive probe as shown in (*B*). (*D*) The fluorescence microscopy image of the sample in the chip highlighted in the white dashed line frame in (*C*) (Scale bar, 300 μm). (*E*) The relationship between fluorescence intensity and reaction time of sample resting in microfluidic chip. (*F*) Calibration curve at 400 nm from the absorption spectrum of potassium titanium oxalate (PTO) solution with added H_2O_2. Abs, absorption. The green star represents the concentration of H_2O_2 generated from the microfluidic chip. The excitation source is a green laser pointer (530 nm).

a function of the contact time between water and the glass substrate. The fluorescence emission intensity was recorded as soon as DI water had filled the channel. The fluorescence intensity increased rapidly, and the maximum value was reached after 10 s. Quantitative analysis of H_2O_2 generation in the microfluidic channel was performed by using potassium titanium oxalate (PTO; $K_2TiO(C_2O_4)_2{\cdot}H_2O$) according to a previously reported method (6, 21). *SI Appendix*, Fig. S4 shows the ultraviolet-visible (UV-vis) absorption spectra of 0.1 M PTO solutions with various concentrations of a standard H_2O_2 solution, and with the sample obtained from the microfluidic chip. The concentration of H_2O_2 in the microfluidic chip was 1.9 mg L^{-1} (Fig. 1*F*).

H_2O_2 Generation at Water–Solid Interface. To investigate the origin of the spontaneous generation of H_2O_2, we observed the H_2O_2 signals from the probe at the water–glass interface as well as the signals in the channel; Fig. 2*A* shows the fluorescence intensity curve. The fluorescence intensity decreased along the normal direction of the glass substrate. The results indicate that the concentration of H_2O_2 at the water–glass interface was much higher than that in the channel. This finding shows that H_2O_2 generation may be dependent on the water–solid interface. Notably, the relationship between the H_2O_2 concentration and the water–solid interface was confirmed by determining the H_2O_2 concentrations in capillary devices with various diameters, as shown in Fig. 2*B* and *SI Appendix*, Fig. S5. The concentrations of H_2O_2 were determined by the ratio of the internal surface area of the capillary device to its volume (surface area/channel volume). The excellent linear relationship between the H_2O_2 concentration and the surface area/channel volume ratio shows that the spontaneous generation of H_2O_2 can be attributed to the effect of the water–solid interface. Notably, the concentration of H_2O_2 generated in the capillary device was of the same order of magnitude as that in the PDMS microfluidic channel. This result further rules out H_2O_2 production caused by radicals generated from newly prepared PDMS in the microfluidic device (22).

Ionic strength and pH have important effects on the water–solid interface, such as the formation of an electric double layer. We therefore investigated the spontaneous generation of H_2O_2 from NaOH, NaCl, and HCl solutions at various concentrations (Fig. 2*C*). The results show that H_2O_2 production decreased with increasing ionic strength. In addition, the concentration of H_2O_2 generated in DI water was higher than that generated in NaOH, NaCl, and HCl solutions. Among these, the NaOH solution had the least inhibitory effect on the spontaneous generation of H_2O_2. These data indicate that the water–solid interface may be the origin of the spontaneous generation of H_2O_2 under these conditions.

H_2O_2 Originates from the Hydroxyl Groups on the Solid Surface. It is important to identify the O-atom source to further understand the effects of the water–solid interface on H_2O_2 production. We considered that possible O-atom sources at the water–solid interface include oxygen-containing groups on the solid substrate and dissolved O_2 in the water. Therefore, we examined the correlation between dissolved O_2 and H_2O_2 production (Fig. 2*D*). The amount of H_2O_2 produced remained at the same level regardless of how the amount of dissolved O_2 was changed. Our observations indicate that the H_2O_2 generated at the water–solid interface was not produced by oxidation with dissolved O_2; this finding was in good agreement with previously reported results for

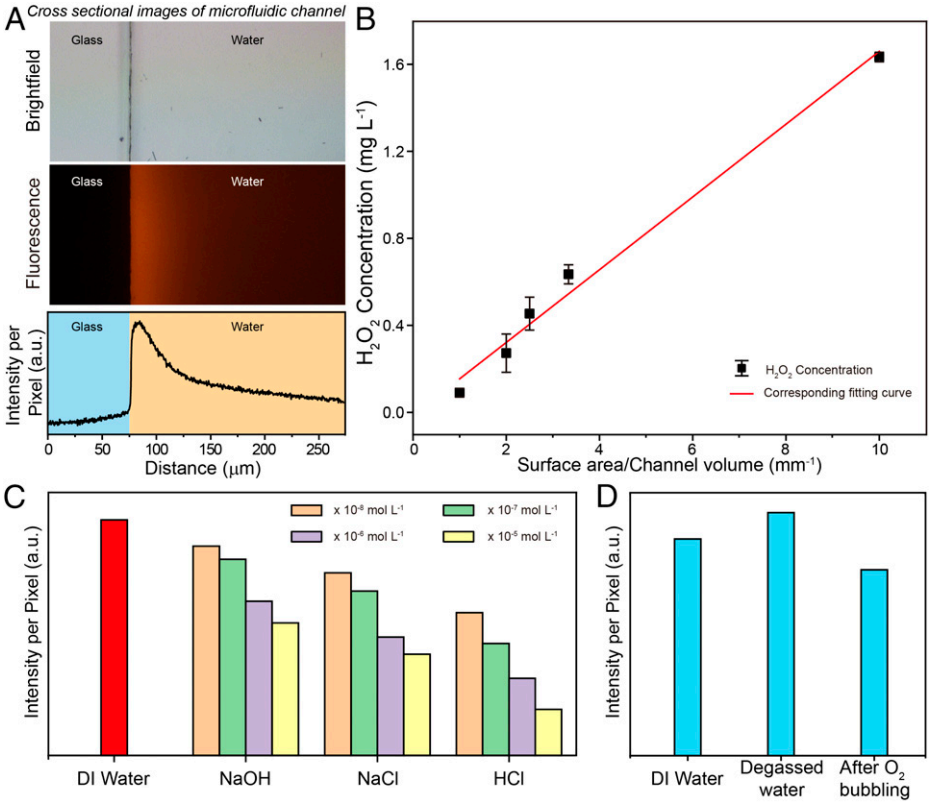

Fig. 2. Spontaneous generation of H_2O_2 at water–solid interface. (*A*) The fluorescent profiles of the spontaneous generation of H_2O_2 along the normal direction of the substrate (*Top*, the optical microscopy image of a typical straight channel; *Middle*, the corresponding fluorescence image; *Bottom*, the corresponding fluorescence intensity). (*B*) The correlation between generated H_2O_2 concentration and surface area/channel volume. Note that the measurements were carried out in capillary devices with various diameters. (*C*) H_2O_2 concentration as a function of different pH values and ionic strengths. (*D*) Dependence of H_2O_2 generation on dissolving different gases in water.

aqueous microdroplets (6, 23). Our results suggest that the O-atom source for H_2O_2 generation may come from oxygen-containing groups on the solid substrate.

We addressed the above issue by investigating the correlation between the density of hydroxyl groups on the substrate and H_2O_2 production. SiO_2 substrates were used to prevent interference from impurity elements in the substrates. The density of hydroxyl groups on the SiO_2 substrate was increased after typical O_2 plasma activation treatment; this was confirmed by using infrared spectroscopy and X-ray photoelectron spectroscopy (XPS) to examine the substrate (*SI Appendix*, Figs. S6 and S7) (24). Fig. 3*A* shows that the fluorescence emission intensity of the H_2O_2-sensitive probe on the substrate treated with O_2 plasma (Fig. 3*A*, *Middle*) was higher than that of the bare glass substrate (Fig. 3*A*, *Top*). This result shows that H_2O_2 production at a water–solid interface can be enhanced by increasing the hydroxyl group density on the solid substrate. The density of hydroxyl groups on the SiO_2 substrate was decreased based on the modification of the substrate with 3-(methacryloyloxy) propyltrimethoxysilane (MPTMS) (*SI Appendix*, Fig. S8) (25). Fluorescence signals were hardly observed on the substrate, which was modified with MPTMS (Fig. 3*A* and *B*, *Bottom*). This result can be attributed to the decrease of the density of hydroxyl groups on the substrate caused by the reaction between the mercapto groups of MPTMS and the hydroxyl groups. Therefore, surface hydroxyl groups on the solid substrate play a key role in H_2O_2 production at the water–solid interface. The disappearance of the fluorescence emission from the H_2O_2-sensitive probe offers solid evidence that the spontaneous generation of H_2O_2 is determined by the presence of surface hydroxyl groups on the solid substrate.

The Use of Isotopic Labeling. We designed an O-atom isotope experiment to further explore the origin of the oxygen atoms for the generation of H_2O_2 (Fig. 3*C*). $^{18}O_2$ plasma treatment was used to create sufficient ^{18}O-labeled hydroxyl groups on the SiO_2 substrate. Spontaneous generation of H_2O_2 and corresponding boronic acid cleavage on the ^{18}O-labeled SiO_2 substrate was performed to determine whether surface hydroxyl groups participate in the reaction at the water–solid interface. If the surface hydroxyl group is the origin of the O atom in the generation of H_2O_2, then the O-atom isotope signals would be observed in 4-hydroxybenzoic acid, as shown in Fig. 3*D*. We therefore compared the 4-hydroxybenzoic acid productions on the SiO_2 substrates treated with O_2 and $^{18}O_2$ plasmas. The intensity of the mass spectrometric peak at 139.04 *m/z* increased after isotope treatment (Fig. 3*E*), which suggests that the O atom in the surface hydroxyl group plays an important role in the mass balance during the reaction. Additional isotope experiments were performed to further confirm the origin of the O atom during H_2O_2 generation. In these experiments, $H_2{}^{18}O$ was used to produce H_2O_2 on a typical SiO_2 substrate and on an ^{18}O-labeled substrate. *SI Appendix*, Figs. S9 and S10 show that the intensity of the peak at 139.04 *m/z* obtained when $H_2{}^{18}O$ was used was slightly lower than that in Fig. 3*E*, whereas the signal observed by using $H_2{}^{18}O$ on the ^{18}O-treated substrate was slightly higher. However, all the peak intensities were of the same order of magnitude. We propose that the ^{18}O signals observed in the $H_2{}^{18}O$ control experiments can be attributed to the rearrangement of O atoms between water molecules absorbed on the SiO_2 surface and the oxide substrate. These observations suggest that the O atoms

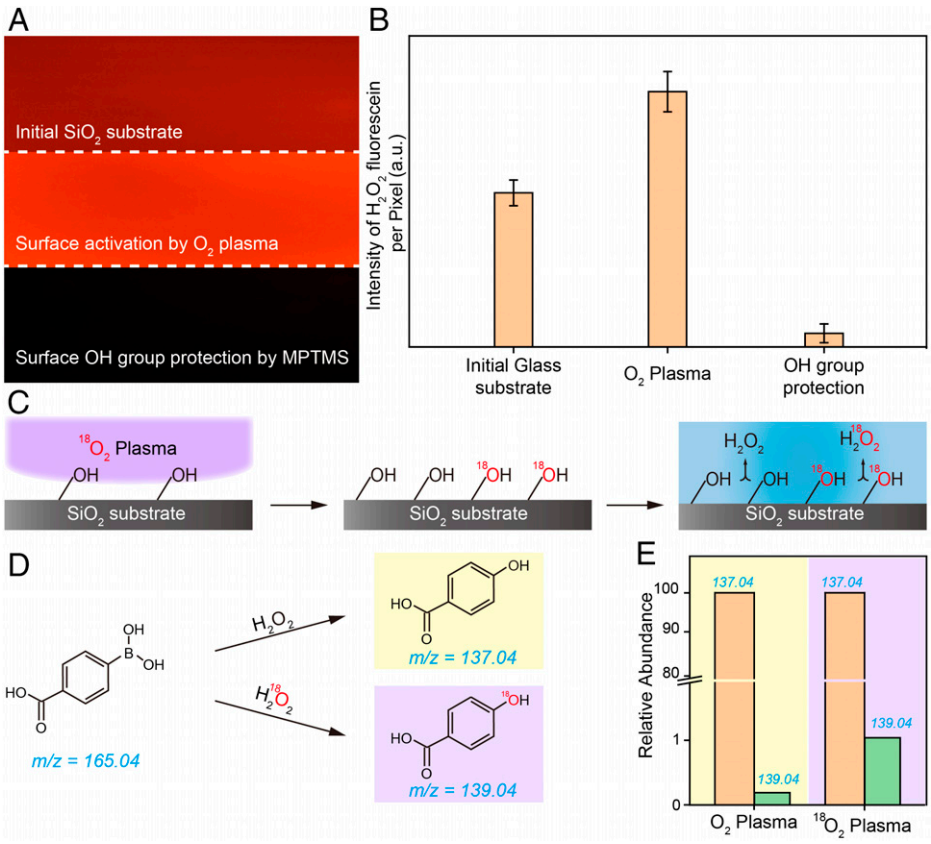

Fig. 3. Dependence of H_2O_2 generation on the surface OH groups on the SiO_2 substrate. (*A*) Fluorescent microscopy images of H_2O_2 generation on SiO_2 substrate with different surface treatments. (*B*) The corresponding fluorescence intensity profiles of H_2O_2 generation in (*A*). (*C*) Schematic of the O-atom isotope experiment setup. (*D*) Reaction scheme of H_2O_2-promoted/$H_2{}^{18}O_2$-promoted deborylation of 4-CPB. (*E*) Mass spectrum analysis of 4-hydroxybenzoic acid on SiO_2 substrates treated by O_2 and $^{18}O_2$ plasmas.

in H_2O_2 generation originate from surface hydroxyl groups on the substrate.

Several previous reports have indicated that hydroxyl radicals can combine to form H_2O_2 in the presence of water (6, 26). We therefore speculated that some of the hydroxyl groups on the solid surface generate hydroxyl radicals during contact between water and the solid surface and then combine to form H_2O_2. To support our speculation, water containing DMSO, which is a typical hydroxyl radical scavenger (27), was injected into the microfluidic channel, followed by a measurement of the H_2O_2 generation. As shown in *SI Appendix*, Fig. S11, it is difficult to detect the fluorescence signal from H_2O_2 in the presence of DMSO. This indicates that the spontaneous generation of H_2O_2 can be predominantly, if not completely, attributed to the recombination of hydroxyl radicals generated from the hydroxyl groups on the solid surface when the solid substrate contacts water.

The generation of hydroxyl radicals from hydroxyl groups is accompanied by electron transfer (28). On the basis of previous investigations of electron transfer in water–solid contact electrification, we assumed that electrons can play a fundamental role in driving the spontaneous generation of H_2O_2. We therefore measured the current flowing from the substrate to the ground when water contacted the substrate and simultaneously observed the fluorescence signal from H_2O_2 generation. *SI Appendix*, Fig. S12 shows that current changes occur in synchronization with the generation of H_2O_2. We also used Kelvin probe force microscopy (KPFM) to determine the surface charge density of the substrate before and after contact with water (*SI Appendix*, Fig. S13). The surface charge density of the substrate changed from 113.5 to -179.7 μC m^{-2}, which suggests that the substrate gained electrons on contact with water. Notably, it was estimated that the H_2O_2 generation reaction in the microfluidic channel would require a maximum of 2×10^{-15} mol electrons, which is one order of magnitude lower than the amount of charge measured during contact. This finding also suggests that the change of the surface charge density when water contacted the substrate may have multiple origins, such as ion transfer, overlap of electron clouds, and surface hydroxyl groups on the substrate (5). We do not know the fate of all the charges detected on the solid surface, but we consider that the charge transfer at the water–solid interface is sufficient to produce H_2O_2.

Mechanism for Spontaneous Generation of H_2O_2 at the Water–Silica Interface. Our experimental results and analysis revealed that the production of H_2O_2 at the water–solid interface originated from the radicals generated from surface hydroxyl groups when water contacted with the solid substrate. We investigated a possible reaction pathway involved in the surface hydroxyl groups. It is well known that hydroxyl groups on the surface of oxides are amphoteric in character (29). Moreover, early research demonstrated that surface acidic hydroxyl groups ($Si\text{-}OH_{(a)}$) contribute most to the generation of hydroxyl radicals (30). Thus, we investigated the correlation between the density of acidic hydroxyl groups on the SiO_2 surface and the generation of H_2O_2 at the water–solid interface. Notably, the density of acidic hydroxyl groups was measured, based on the reaction between NaOH and the acidic hydroxyl groups reported previously (31). The density of acidic hydroxyl groups on SiO_2 substrates fabricated under the same conditions in Fig. 3*B* is shown in *SI Appendix*, Fig. S14. We observed that the density of the acidic surface hydroxyl groups on SiO_2 treated by O_2 plasma was higher than the other two substrates. Next, the concentration of H_2O_2 generated on those substrates was recorded (shown in Fig. 4*A*). The linear relationship between H_2O_2 concentration and the density of acidic surface hydroxyl groups was in good agreement with the results in Fig. 2*B*. More importantly, we compared the density of the acidic surface hydroxyl groups before and after H_2O_2 generation. As shown in Fig. 4*B*, the density of the acidic surface hydroxyl groups decreased after the production of H_2O_2, which offers solid evidence that acidic hydroxyl groups act as a starting reactant in the pathway of H_2O_2 generation. Notably, acidic surface hydroxyl groups ($Si\text{-}OH_{(a)}$) may be ionized in water to generate hydronium cations and silanolate anions ($Si\text{-}O^-$). Thus, $Si\text{-}O^-$ groups are thought to be the initial source of O atoms to form H_2O_2 during the contact electrification process:

$$Si - OH_{(a)} + H_2O \rightarrow Si - O^- + H_3O^+ \quad [1]$$

When contact occurs between the SiO_2 surface and water molecules, the electron may transfer from H_2O to the solid surface (32) and thus form H_2O during this process. We tested the amount of H_2O_2 generated on the surface of SiO_2 depending on different temperatures. In order to meet the detection limit requirements, we used SiO_2 powder in contact with humid air to create a solid–liquid interface with a sufficiently large area for further investigation. As shown in Fig. 4*C*, there was an increase in H_2O_2 production with increasing temperature. This result could be attributed to the kinetic energy increase caused by the rising temperature, which might enhance the probability of the contact between water molecules and the SiO_2 surface and thus increase the probability of electron transfer. Moreover, the signal of H_2O_2 cannot be detected when the temperature is below 5 °C. This result might be ascribed to the kinetic energy of water molecules, which is too low to generate enough electrons during contact electrification for the generation of detectable amounts of H_2O_2. A possible reaction pathway can be written as follows:

$$H_2O \rightarrow H_2O^+ + e^- \quad [2]$$

Typically, $Si\text{-}^{18}O^-$ ions can work as a base to accelerate some reactions by promoting the stoichiometric deprotonation step (33, 34).

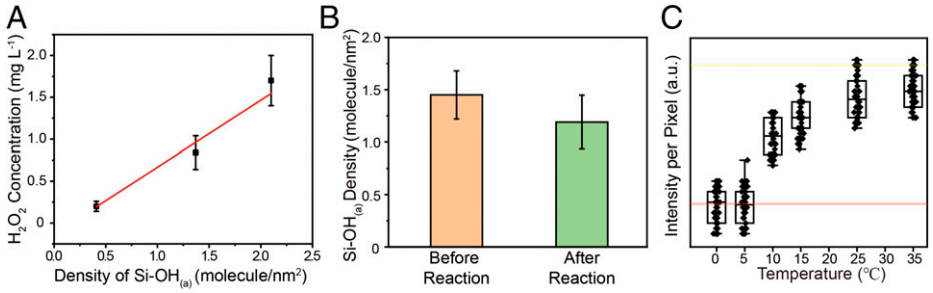

Fig. 4. Correlation between $Si\text{-}O^-$ groups and H_2O_2 generation. (*A*) Dependence of the H_2O_2 concentration on the density of $Si\text{-}O^-$ groups. (*B*) Comparation of $Si\text{-}OH_{(a)}$ density before and after H_2O_2 generation. (*C*) Temperature dependence of H_2O_2 generation. The pink line is fluorescence intensity per pixel of 5 mL aqueous PTO solution without added H_2O_2. The yellow line is fluorescence intensity per pixel of 5 mL aqueous PTO solution with added 0.1 g SiO_2 powder and 0.5 mg H_2O_2.

$Si\text{-}^{18}O^-$ ions could react with H_2O^+ to form hydroxyl radicals during the contact electrification process:

$$Si-{}^{18}O^- + H_2O^+ \rightarrow Si-OH + {}^{18}OH\bullet \quad [3]$$

Then, a hydroxyl radical recombination could yield $H_2{}^{18}O_2$:

$${}^{18}OH\bullet + {}^{18}OH\bullet \rightarrow H_2{}^{18}O_2 \quad [4]$$

In fact, our proposed mechanism is built around the hypothesis that the overlap between the electron clouds of the water molecule and the solid surface during the contact will lead to the generation of H_2O^+ and OH•. However, various intermediates present in the above reaction pathway are difficult to test, so we believe that the mechanism of the spontaneous generation of H_2O_2 at the water–solid interface is still an open issue that requires further in-depth research.

In addition, we believe that the generation of H_2O_2 at the water–solid interface may provide a perspective on a physicochemical process similar to that in the microdroplet. We assume that the electron will transfer from one H_2O molecule to another H_2O molecule during their contact and that hydroxyl radicals may generate during the contact electrification. Thus, the generation of H_2O_2 at the water–solid interface is in good agreement with that at the surface of the microdroplets.

Universality of H_2O_2 Generation from Water Contact Electrification. The universality of this phenomenon was investigated by observing the spontaneous generation of H_2O_2 on nine other types of substrates. As shown in *SI Appendix*, Fig. S15*A*, similar phenomena were observed on various substrates. In addition, we carried out a set of comparative experiments to investigate the changes of the surface charge before and after water–solid contact by using zeta potential measurements. *SI Appendix*, Fig. S16 shows the difference in zeta potential before and after the contact between water and these powder samples. It can be observed that the trend of the zeta potential difference depended on solids species in a manner consistent with the trend of the H_2O_2 generation on their surfaces. This result provides further proof of the importance of contact electrification in causing H_2O_2 production at the water–solid interface. More importantly, we tested the generation of H_2O_2 on the surfaces of standard soil (GBW07446) and atmospheric fine particles of 2.5 μm or smaller ($PM_{2.5}$) after they had been placed in an oven at room temperature (25 °C) at various relative humidities. *SI Appendix*, Fig. S15*B* shows that H_2O_2 generation increased with increasing relative humidity, which is in good agreement with a previous literature report (35). To rule out in situ catalytic processes in the soil, we also investigated H_2O_2 generation on O_2 plasma–activated and MTPMS-modified soil particles, respectively. The H_2O_2 generation yield was affected by changing the density of the hydroxyl groups on the surface of the soil. *SI Appendix*, Fig. S15*C* shows that H_2O_2 spontaneous generation also occurred at the surfaces of $PM_{2.5}$ particles at various different values of the relative humidity. Note that the composition of atmospheric fine particles is very complex. Several publications have reported that the main components of China's atmospheric fine particles include carbon black, nitrate, sulfate, and ammonium salt (36, 37). We carried out an energy dispersive X-say spectroscopy measurement to analyze the main elements contained in our atmospheric fine particles sample. As shown in *SI Appendix*, Fig. S17, the main elements were C, N, S, and O. We believe that the composition of atmospheric fine particles is similar to that reported previously (37). The generation of H_2O_2 on the surface of $PM_{2.5}$ particles could be attributed to their surface hydroxyl groups and contact between water and their surface. The results of this study may therefore help us understand the mechanism of H_2O_2 generation in the environment and explain how nature behaves, such as the seasonality of viral respiratory infections (38). In addition, we have considered a recent report (34) that glass surfaces can act as heterogeneous catalysts to accelerate various base-catalyzed reactions. The present study may help us further understand the heterogeneous catalytic reaction at the solid–water interface and design interfacial catalysts to replace homogeneous catalysts that need to be dispersed in the bulk phase.

Conclusions

In summary, our experimental and modeling results provide direct evidence for the spontaneous generation of H_2O_2 at water–solid interfaces from hydroxyl groups on the solid surface. These observations give a perspective on water–solid interactions and enhance our understanding of water–solid contact electrification. The identification of H_2O_2 generation from the surfaces of solid and atmospheric fine particle samples shows the possibilities of developing mechanisms for pollutant degradation and transformation in the environment. When combined with materials with high catalytic activities, these phenomena could have important applications in catalytic chemistry.

Materials and Methods

Materials. Unless otherwise stated, HCl (AR, Sinopharm Chemical Reagent Co., Ltd, China), NaOH (AR, Sinopharm Chemical Reagent Co., Ltd, China) NaCl (AR, Sinopharm Chemical Reagent Co., Ltd, China), O_2 (99.999%, Wuhan Iron and Steel Group Gas Co., Ltd., China); heavy O_2 (99.99%, Wuhan Niuruide Gas Co., Ltd., China), PTO dihydrate (99.99%, Sigma-Aldrich, USA); 4-CPB (99.99%, Sigma-Aldrich, USA); anhydrous dimethyl sulfoxide (99.99%, Sigma-Aldrich, USA); 10-acetyl-3,7-dihydroxyphenoxazine (KeyGEN BioTECH Co., Ltd, China); H_2O standard solution (1,000 μg/mL, Beijing Northern Weiye Metrology Research Institute, China); PDMS prepolymer RTV 615 (Momentive, USA); graphite powder; CaO; ZrO; SiO_2; Al_2O_3; MnO_2, TiO_2; CuO; ZnO (Shanghai Aladdin Bio-Chem Technology Co., Ltd, China); and standard soil (GBW07446, China) were used in experiments. DI water (Merck Millipore, USA) was used in all experiments. SiO_2 substrates (optical grade, Sigma-Aldrich, USA), conductive glass substrates (NSG Pilkington FTO glass), and glass substrates (Jiangsu Fanchuan Co., Ltd, China) were ultrasonically cleaned with acetone, ethanol, and DI water for 30 min before use.

Fabrication of Microchannel Structure Devices. The channel layout was drawn by L-edit software, and the mask was prepared by ultraviolet direct writing equipment. Subsequently, relief microchannels were built on the Si wafer by photolithography. The cylindrical channel (1.5 mm diameter) had a total length of 2 cm, a width of 100 μm, and a height of 20 μm. The PDMS prepolymer and the curing agent were mixed in a 9:1 mass ratio and then poured onto the silicon wafer with relief microchannel structure, decompressed and defoamed, and heat-treated at 80 °C for 30 min, and finally PDMS with a microchannel structure was obtained. To fabricate microchannel structured devices, holes were opened in the reserved position, and then PDMS monolith was attached to the clean glass substrate. A pressure of 0.1 MPa was applied externally and kept at 85 °C for 30 min to ensure stable bonding between PDMS and the glass substrate.

Qualitative Characterization of H_2O_2. 10-acetyl-3,7-dihydroxyphenoxazine was used in the experiments as a fluorescent indicator of H_2O_2. 1 mM 10-acetyl-3,7-dihydroxyphenoxazine aqueous solution was pumped into the microchannel at a flow rate of 20 μL h^{-1}, and the monolithic device was placed under an inverted fluorescence microscope for observation. A 530 nm laser was applied as an excitation light source, the exposure time was fixed, and the change the overall fluorescence intensity in the channel was recorded. The device was placed under a microscope on its side to observe the diffusion of H_2O_2 from the glass surface. All fluorescence images were calculated using Image J software to obtain the average fluorescence intensity under different conditions.

To observe the effect of ionic strength on the formation of H_2O_2, 1 mM 10-acetyl-3,7-dihydroxyphenoxazine was added to DI water and different concentrations (10^{-5},10^{-6},10^{-7} and 10^{-8} Mol L^{-1}) of HCl, NaCl, and NaOH solution, respectively. Different solutions were pumped into the microchannel at a flow rate of 20 μL h^{-1}, and the maximum fluorescence intensity was recorded. The fluorescence intensity of DI water was used as the standard to qualitatively explore the relationship between ionic intensity and H_2O_2 generation.

To investigate the effect of dissolved O_2 in the solution on the formation of H_2O_2, deionized water was degassed and aerated. Deionized water was continuously boiled for 30 m to achieve degassing, and another set of deionized water was continuously bubbled with O_2 for 1 h to ensure higher dissolved O_2 content. Untreated DI water was used as a control group, and 1 mM 10-acetyl-3,7-dihydroxyphenoxazine was added to the three groups of DI water, which were pumped into the microchannel, and the maximum fluorescence intensity was recorded.

Quantitative Characterization of H_2O_2. The color reaction of PTO with H_2O_2 was considered as one of the methods to quantitatively characterize the concentration of H_2O_2. H_2O_2 solutions of 1, 2, 3, 4, and 5 mg L^{-1} were prepared using a H_2O_2 standard solution and were mixed with 0.3 M PTO solution in a volume ratio of 1:1. The mixed solution was detected by a UV-vis spectrometer (UV-2550, Shimadzu, Japan), the absorbance at 400 nm was taken as the characteristic value, and the standard curve was drawn according to the concentration of corresponding H_2O_2.

The DI water was pumped through the microchannel at 20 μL h^{-1} and then mixed with 0.3 M PTO solution by equal volume, and then its absorbance was measured by a UV-vis spectrometer. The absorbance at 400 nm was compared to the standard curve, and the concentration of H_2O_2 in deionized water was finally calculated.

To further explore the relationship between the concentration of H_2O_2 and the solid–liquid interface, capillaries with different diameters were used as experimental objects. First, 1 mM 10-acetyl-3,7-dihydroxyphenoxazine solution was pumped into different-diameter (50, 150, 200, 250, and 500 μm) capillaries at different flow rates, respectively. The flow rates of DI water pumped into the different capillaries were 20, 120, 320, 500, and 2,000 μL h^{-1}, which ensured that the solution was advancing at the same rate in the capillaries. Then 0.5 mL DI water was collected at the exit of the capillary, mixed with 0.3 M PTO solution by equal volume, and its absorbance at 400 nm was measured by a UV-vis spectrometer and compared to the standard curve; finally, the concentration was calculated.

Effects of Surface Hydroxyl Groups on H_2O_2 Generation. XPS and a Fourier transform infrared spectrophotometer (Bruker) were used to characterize the surface group changes of glass substrates after O_2 plasma treatment. XPS was performed on a multifunctional imaging electron spectrometer (ESCALAB 250XI, Thermo) using monochromatized Al K_a radiation (1486.6 eV).

The potential changes of the glass substrate surface before and after the flow of DI water were obtained by (KPFM) experiments. Experiments were performed on a commercial atomic force microscope (AFM) instrument (Multimode 8 Bruker, USA). AFM probe (NSC18, Mikro-Mash, USA; Au coated; tip radius: 25 nm; spring constant: 2.8 N m^{-1}) was used as the conductive tip. At the same time, we also used conductive glass as the substrate and cooperated with the electrochemical workstation to detect the drop of DI water on the O_2 plasma-treated substrate and to record the change of the current.

To investigate the effect of surface hydroxyl groups on the formation of H_2O_2, O_2 plasma was used to increase the surface hydroxyl groups and MPTMS was used to reduce the surface hydroxyl groups. An untreated glass substrate was used as the control. Next, 20 μL 1 mM 10-acetyl-3,7-dihydroxyphenoxazine solution was added dropwise to three different glass substrates, and the fluorescence images were recorded under an inverted fluorescence microscope; finally, the mean fluorescence intensity was calculated using Image J.

Next, 100 μM 4-CPB solution was pumped through the microchannel at 20 μL h^{-1} and a 0.5 mL sample was collected at the outlet. The samples were analyzed using liquid chromatography-mass spectrometry in negative mode, and 4-CPB, 4-carboxyphenol, 4,4′-oxybis (benzoic acid), and boric acid were observed separately. The relative abundance of 4-hydroxybenzoic acid remained low, which may have been caused by low turnover resulting from poor ionization efficiency or short reaction times when no voltage was applied.

To explore the source of O atoms during H_2O_2 generation, a $H_2{}^{18}O$ mixture and $H_2{}^{18}O$ water were used in the experiments. The microchannels were treated with O_2 plasma and $^{18}O_2$ plasma, respectively, for 20 min before bonding. Then 100 μM 4-CPB solution was pumped through the microchannel. In addition, 4-boxyphenylboronic acid was dissolved in $H_2{}^{18}O$ to conduct experiments, and the samples at the outlet were analyzed using high-resolution liquid chromatography-mass spectrometry, and the intensity changes of 137 *m/z* and 139 *m/z* corresponding to 4-carboxyphenol were compared.

The Boehm titration method was used to determine the hydroxyl density of the material surface. The silica glass was cut into a 0.5 × 0.5 cm square and a 2 g sample was dissolved into 25 mL anhydrous ethanol, followed by adding 75 mL of 20 wt% NaCl solution. The solution was stirred slowly and a pH meter (Mettler, SevenExcellence) was used to detect the overall pH change of the solution in real time. The pH of the solution was adjusted to 4 with 0.1 M HCl. After the pH was stabilized, 0.1 M NaOH solution was slowly added dropwise to bring the pH of the solution back to 9 and the amount of NaOH was recorded. The number of hydroxyl groups per square nanometer (N) on the surface of the material was calculated according to the following equation:

$$N = \frac{CVN_A \times 10^{-3}}{S}$$

where C is the concentration of NaOH (mol/L), V (mL) is the volume of NaOH consumed as the pH rises from 4 to 9, N_A is Avogadro's constant, and S is the surface area of the sample.

Additional Information. The formation of H_2O_2 on the surface of natural materials is presented in the *SI Appendix*.

Data Availability. All study data are included in the article, the *SI Appendix*, and the publicly available link: https://github.com/RichardZare/Contact_Electrification_PNAS_Data_Repository.

ACKNOWLEDGMENTS. This work is financially supported in part by grants from the Strategic Priority Research Program of the Chinese Academy of Sciences (XPDB2005), the National Nature Science Foundation of China (22193051, 22193052, 22136006, 21705057), the National Key Research and Development Program of China (2020YFA0907400), and the Youth Talent Support Program of Jianghan University. R.N.Z. acknowledges support from the US Air Force Office of Scientific Research through the Multidisciplinary University Research Initiative program (AFOSR FA9550-21-1-0170). We thank Professor P. Wang, Hong Kong Polytechnic University, Z. Q. Tian, Xiamen University, A. Colussi, California Institute of Technology, and D. Ben-Amotz, Purdue University, for helpful discussions.

Author affiliations: [a]State Key Laboratory of Precision Blasting, Jianghan University, Wuhan, 430056, China; [b]Hubei Key Laboratory of Environmental and Health Effects of Persistent Toxic Substances, Jianghan University, Wuhan, 430056, China; [c]State Key Laboratory of Environmental Chemistry and Ecotoxicology, Research Center for Eco-Environmental Sciences, Chinese Academy of Sciences, Beijing 10085, China; [d]School of Physics and Technology, Wuhan University, Wuhan, 430072, China; [e]Institute for Interdisciplinary Research, Jianghan University, Wuhan 430056, China; and [f]Department of Chemistry, Stanford University, Stanford, CA 94305

1. S. Lin, X. Chen, Z. L. Wang, Contact electrification at the liquid-solid interface. *Chem. Rev.* **122**, 5209–5232 (2022).
2. M. Matsui, N. Murasaki, K. Fujibayashi, P. Y. Bao, Y. Kishimoto, Electrification of pure water flowing down a trough set up with a resin sheet. *J. Electrost.* **31**, 1–10 (1993).
3. K. Yatsuzuka, Y. Mizuno, K. Asano, Electrification phenomena of pure water droplets dripping and sliding on a polymer surface. *J. Electrost.* **32**, 157–171 (1994).
4. K. Yatsuzuka, Y. Higashiyama, K. Asano, Electrification of polymer surface caused by sliding ultrapure water. *IEEE Trans. Ind. Appl.* **32**, 825–831 (1996).
5. D. Ben-Amotz, Electric buzz in a glass of pure water. *Science* **376**, 800–801 (2022).
6. S. Lin, L. Xu, A. C. Wang, Z. L. Wang, Quantifying electron transfer in liquid-solid contact electrification and the formation of electric double-layer. *Nat. Commun.* **11**, 399 (2020).
7. J. K. Lee *et al*., Spontaneous generation of hydrogen peroxide from aqueous microdroplets. *Proc. Natl. Acad. Sci. U.S.A.* **116**, 19294–19298 (2019).
8. D. Gao, F. Jin, J. K. Lee, R. N. Zare, Aqueous microdroplets containing only ketones or aldehydes undergo Dakin and Baeyer-Villiger reactions. *Chem. Sci. (Camb.)* **10**, 10974–10978 (2019).

9. J. K. Lee *et al.*, Condensing water vapor to droplets generates hydrogen peroxide. *Proc. Natl. Acad. Sci. U.S.A.* **117**, 30934–30941 (2020).
10. M. T. Dulay *et al.*, Spraying small water droplets acts as a bacteriocide. *QRB Discovery* **1**, e3 (2020).
11. A. Gallo Jr. *et al.*, On the formation of hydrogen peroxide in water microdroplets. *Chem. Sci. (Camb.)* **13**, 2574–2583 (2022).
12. T. Kakeshpour, B. Metaferia, R. N. Zare, A. Bax, Quantitative detection of hydrogen peroxide in rain, air, exhaled breath, and biological fluids by NMR spectroscopy. *Proc. Natl. Acad. Sci. U.S.A.* **119**, e2121542119 (2022).
13. M. A. Mehrgardi, M. Mofidfar, R. N. Zare, Sprayed water microdroplets are able to generate hydrogen peroxide spontaneously. *J. Am. Chem. Soc.* **144**, 7606–7609 (2022).
14. D. Nguyen, S. C. Nguyen, Revisiting the effect of the air–water interface of ultrasonically atomized water microdroplets on H_2O_2 formation. *J. Phys. Chem. B* **126**, 3180–3185 (2022).
15. S. Lin *et al.*, Electron transfer in nanoscale contact electrification: Effect of temperature in the metal-dielectric case. *Adv. Mater.* **31**, e1808197 (2019).
16. C. Xu *et al.*, On the electron-transfer mechanism in the contact-electrification effect. *Adv. Mater.* **30**, e1706790 (2018).
17. Z. Wang *et al.*, Contact-electro-catalysis for the degradation of organic pollutants using pristine dielectric powders. *Nat. Commun.* **13**, 130 (2022).
18. W. Xu *et al.*, A droplet-based electricity generator with high instantaneous power density. *Nature* **578**, 392–396 (2020).
19. N. Kavokine, M. L. Bocquet, L. Bocquet, Fluctuation-induced quantum friction in nanoscale water flows. *Nature* **602**, 84–90 (2022).
20. J. G. Mohanty, J. S. Jaffe, E. S. Schulman, D. G. Raible, A highly sensitive fluorescent micro-assay of H_2O_2 release from activated human leukocytes using a dihydroxyphenoxazine derivative. *J. Immunol. Methods* **202**, 133–141 (1997).
21. M. H. Kastvig *et al.*, Effect of humidity on cellulose pellets loaded with potassium titanium oxide oxalate for detection of hydrogen peroxide vapor in powders. *Power Tech.* **366**, 348–357 (2020).
22. H. T. Baytekin, B. Baytekin, B. A. Grzybowski, Mechanoradicals created in "polymeric sponges" drive reactions in aqueous media. *Angew. Chem. Int. Ed. Engl.* **51**, 3596–3600 (2012).
23. F. Collin, Chemical basis of reactive oxygen species reactivity and involvement in neurodegenerative diseases. *Int. J. Mol. Sci.* **20**, E2407 (2019).
24. Z. Liu, N. M. D. Brown, A. McKinley, Characterization of oxygen plasma-modified mica surfaces using XPS and AFM. *Appl. Surf. Sci.* **108**, 319–332 (1997).
25. J. Wu *et al.*, Surface modification of nanosilica with 3-mercaptopropyl trimethoxysilane: Experimental and theoretical study on the surface interaction. *Chem. Phys. Lett.* **591**, 227–232 (2014).
26. S. Du, J. S. Francisco, S. Kais, Study of electronic structure and dynamics of interacting free radicals influenced by water. *J. Chem. Phys.* **130**, 124312 (2009).
27. R. V. Panganamala, H. M. Sharma, R. E. Heikkila, J. C. Geer, D. G. Cornwell, Role of hydroxyl radical scavengers dimethyl sulfoxide, alcohols and methional in the inhibition of prostaglandin biosynthesis. *Prostaglandins* **11**, 599–607 (1976).
28. L. Zhao *et al.*, Sprayed water microdroplets containing dissolved pyridine spontaneously generate pyridyl anions. *Proc. Natl. Acad. Sci. U.S.A.* **119**, e2200991119 (2022).
29. H. P. Boehm, Acidic and basic properties of hydroxylated metal oxide surfaces. *Discuss. Faraday Soc.* **52**, 264–275 (1971).
30. W. Li *et al.*, Relationship between surface hydroxyl groups and liquid-phase photocatalytic activity of titanium dioxide. *J. Colloid Interface Sci.* **444**, 42–48 (2015).
31. I. I. Salame, T. J. Bandosz, Surface chemistry of activated carbons: Combining the results of temperature-programmed desorption, Boehm, and potentiometric titrations. *J. Colloid Interface Sci.* **240**, 252–258 (2001).
32. Z. L. Wang, A. C. Wang, On the origin of contact-electrification. *Mater. Today* **30**, 34–51 (2019).
33. Y. Li, T. F. Mehari, Z. Wei, Y. Liu, R. G. Cooks, Reaction acceleration at solid/solution interfaces: Katritzky reaction catalyzed by glass particles. *Angew. Chem. Int. Ed. Engl.* **60**, 2929–2933 (2021).
34. Y. Li, K. H. Huang, N. M. Morato, R. G. Cooks, Glass surface as strong base, "green" heterogeneous catalyst and degradation reagent. *Chem. Sci. (Camb.)* **12**, 9816–9822 (2021).
35. M. T. Dulay *et al.*, Effect of relative humidity on hydrogen peroxide production in water droplets. *QRB Discovery* **2**, e8 (2021).
36. L. Liu, J. Zhang, R. Du *et al.*, Chemistry of atmospheric fine particles during the COVID-19 pandemic in a megacity of eastern China. *Geophys. Res. Lett.* **48**, 2020GL091611 (2021).
37. Q. Yuan *et al.*, Atmospheric fine particles in a typical coastal port of Yangtze River Delta. *J. Environ. Sci. (China)* **98**, 62–70 (2020).
38. A. Davidse, R. N. Zare, Effect of relative humidity in air on the transmission of respiratory viruses. *Front. Mol. J.* **5**, 5–16 (2021).